

## Article

# Thermal Effect on the Bioconvection Dynamics of Gravitactic Microorganisms in a Rectangular Cavity

Rubén Mil-Martínez <sup>1</sup>, René O. Vargas <sup>2,\*</sup>, Juan P. Escandón <sup>2</sup>, Ildebrando Pérez-Reyes <sup>3</sup>, Marcos Turcio <sup>4</sup>, Aldo Gómez-López <sup>5</sup> and Francisco López-Serrano <sup>6</sup>

- <sup>1</sup> Escuela Militar de Ingenieros, Universidad del Ejército y Fuerza Aérea, Av. Industria Militar No. 261, Col. Lomas de San Isidro, Naucalpan de Juárez 53960, Estado de México, Mexico; rmilm1400@alumno.ipn.mx
- <sup>2</sup> Departamento de Termofluidos, SEPI-ESIME Unidad Azcapotzalco, Instituto Politécnico Nacional, Av. de las Granjas No. 682, Col. Santa Catarina, Alcaldía Azcapotzalco 02250, Ciudad de México, Mexico; jescandon@ipn.mx
- <sup>3</sup> Facultad de Ciencias Químicas, Universidad Autónoma de Chihuahua, Circuito Universitario s/n, Chihuahua 31125, Chihuahua, Mexico; ildebrando3@gmail.com
- <sup>4</sup> Departamento de Ciencias Básicas, Tecnológico Nacional de México Campus Querétaro, Av. Tecnológico s/n, Centro, Santiago de Querétaro 76000, Querétaro, Mexico; heldenklage@live.com.mx
- <sup>5</sup> Departamento de Ingeniería, Sección Mecánica, FES Cuautitlán, Universidad Nacional Autónoma de México, Av. Teoloyucan Km 2.5, Col. San Sebastián Xhala, Cuautitlán Izcalli 54714, Estado de México, Mexico; aldo009.gl@gmail.com
- <sup>6</sup> Departamento de Ingeniería Química, Facultad de Química, Universidad Nacional Autónoma de México, Ciudad de México 04510, Ciudad de México, Mexico; lopezserrano@unam.mx
- \* Correspondence: rvargasa@ipn.mx; Tel.: +52-55-5729-6000 (ext. 64511)



**Citation:** Mil-Martínez, R.; Vargas, R.O.; Escandón, J.P.; Pérez-Reyes, I.; Turcio, M.; Gómez-López, A.; López-Serrano, F. Thermal Effect on the Bioconvection Dynamics of Gravitactic Microorganisms in a Rectangular Cavity. *Fluids* **2022**, *7*, 113. <https://doi.org/10.3390/fluids7030113>

Academic Editor: Michael W. Plesniak

Received: 29 January 2022

Accepted: 15 March 2022

Published: 17 March 2022

**Publisher's Note:** MDPI stays neutral with regard to jurisdictional claims in published maps and institutional affiliations.



**Copyright:** © 2022 by the authors. Licensee MDPI, Basel, Switzerland. This article is an open access article distributed under the terms and conditions of the Creative Commons Attribution (CC BY) license (<https://creativecommons.org/licenses/by/4.0/>).

**Abstract:** In this work, the dynamics of the bioconvection process of gravitactic microorganisms enclosed in a rectangular cavity, is analyzed. The dimensionless cell and energy conservation equations are coupled with the vorticity-stream function formulation. Then, the effects of the bioconvection Rayleigh number and the heating source on the dynamics of microorganisms are discussed. The results based in streamlines, concentration and temperature contours are obtained through numerical simulations considering eight different configurations of symmetrical and asymmetrical heat sources. It is concluded that microorganisms accumulate in the warmer regions and swim through the cooler regions to reach the surface. They form cells for each heat source, but at high concentrations, they form a single stable cell. The results presented here can be applied to control and to understand the dynamics of microorganisms with discrete heat sources.

**Keywords:** bioconvection; gravitactic microorganisms; dynamics of microorganisms; numerical simulation

## 1. Introduction

The bioconvection phenomenon is a wide field of research nowadays. Different applications are indentified to bioconvection such as biological systems [1]. It is crucial to analyze the main factors that influence the patters' behavior formed by the swimming microorganisms produced by a different stimuli. Kuznetsov [2] analyzed the effect of vibration on the stability of a suspension of negatively geotactic microorganisms, in a fluid layer of finite depth. According to his results, at a high-frequency vibration, there is an effect of stabilization of bioconvection. Suggesting that, the high-frequency can be used as a control of bioconvection in laboratory experiments. Kuznetsov [3] studied the onset of thermo-bioconvection in a dilute suspension of oxytactic microorganisms. Here, a shallow fluid layer of the suspension heated from below resulted to be less stable than under isothermal conditions. Alloui et al. [4], investigated the effect of heating or cooling from below, on the stability of a suspension of motile gravitactic microorganisms, in a shallow fluid layer. They found that the thermal effects may either stabilize or destabilize

the suspension and decrease or increase the wavelength of the bioconvective pattern. Nield and Kuznetsov [5] applied linear stability analysis on the onset of bioconvection in a horizontal layer of fluid, containing a suspension of motile microorganisms, with heating or cooling from below. They found that the stability boundary depends on the values of the Lewis and Prandtl numbers and the oscillatory convection could be the favored mode of instability when the layer is heating from the bottom. The change in a favored mode from monotonic to oscillatory is accompanied by a jump to a smaller value of the wavenumber and a jump in frequency from zero to a finite nonzero value. In addition, the relationship between the Rayleigh and the gyrotactic numbers was found. Alloui et al. [6] investigated the effect of heating or cooling from below, of a square enclosure, on the development of gravitactic bioconvection. Here, the influence of thermo-effects on a bifurcation diagram and the flow structure were presented, reporting that the heating from below destabilizes the suspension and cooling from below stabilizes it. Taheri and Bilgen [7] investigated the effect of heating or cooling from below, at constant temperature and constant heat flux, on the development of gravitactic bioconvection in vertical cylinders with stress free sidewalls. They presented that the influence of the thermal effect on the bifurcation diagram and on the pattern of gravitactic bioconvection. They reported that, heating or cooling from below, at constant temperature and constant heat flux, the pattern formation of the gravitactic bioconvection is considerably modified. Niu et al. [8] studied the buoyancy-driven convection of a viscoelastic fluid, saturated in an open-top porous square box, based in a modified Darcy's law. They determined the critical Darcy–Rayleigh number using linear stability analysis. They reported that a high relaxation time destabilizes and produces bifurcation of the flow pattern, while high retardation time stabilizes and postpone the bifurcation of the flow, in the porous medium. Kuznetsov [9] developed a theory of bio-thermal convection in a suspension containing two species of microorganisms, gyrotactic and oxytactic, exhibiting different taxes. He found one traditional Rayleigh number and two bioconvection Rayleigh numbers for gyrotactic and oxytactic microorganisms. Increasing any of the three Rayleigh numbers decreases the stability of the system. Xun et al. [10] investigated the bioconvection between two rotating plates immersed in a nanofluid, with temperature dependent viscosity and thermal conductivity. Their results show that the viscosity variation parameter provokes a remarkable influence on the local skin friction coefficient and the Sherwood number, the local Nusselt number and the wall motile microorganisms flux are more sensitive to the thermal conductivity parameter variation. The aggregation of the motile microorganisms is presented in the middle of the two plates for a higher bioconvection Peclet number. Khan et al. [11] studied the steady two-dimensional boundary layer flow of Burgers bioconvection nanofluid, containing nanoparticles and gyrotactic microorganisms. They determined that the magnitude of the mass transfer rate of microorganisms augments the Peclet number and the microorganisms concentration difference parameter is enhanced. Ramzan et al. [12] studied the heat and mass transfer of a nanofluid with motile gyrotactic microorganisms. They explored the influence of non-linear radiation, viscous dissipation and Joule heating on the motile density of microorganisms. Saini et al. [13] investigated bio-thermal convection in a suspension containing gravitactic microorganisms, saturated by a fluid within the framework of linear and nonlinear stability theory. They determined that the bioconvection Rayleigh number destabilizes the onset of biothermal convection and this effect is more predominant at high microorganisms' speed. Zhao et al. [14] applied a linear stability analysis to investigate the stability of bioconvection, in a suspension of randomly swimming gyrotactic microorganisms, with heated from below. They reported that the Lewis number has no effect on the critical value of thermal Rayleigh number, but has a great influence on the critical bioconvection Rayleigh number. Saini and Sharma [15] presented the effect of vertical throughflow on the onset of nanofluid thermo-bioconvection, in a porous media containing gravitactic microorganisms. They found that the critical wave number is the function of bioconvection, the nanofluid and throughflow parameters. They also found that vertical throughflow disturbs the formation of the bioconvection pattern,

which are necessary for the development of bioconvection. Jabrane et al. [16] studied the influence of the presence of phototactic microorganisms on thermal bioconvection in horizontal porous annulus.

In a previous publication, Mil-Martínez et al. [17] presented the bioconvection of gravitactic microorganisms in a rectangular cavity, through linear analysis and numerical simulation. They reported that the dynamic microorganisms' behavior is influenced by the initial spatial distribution. The stability of the system is dependent on the horizontal wave component that is inversely related to wavelength. The pattern length and the instability of the process are associated with the horizontal component of the wave number and the characteristic wavelength, respectively. In this work, we analyze the effect of the temperature on the dynamics of the gravitactic bioconvection process using eight different heating configurations in a rectangular cavity. To the authors' knowledge, there are no studies that analyze the influence of discrete heat sources on the orientation and spatial distribution of microorganisms in the bioconvective process.

### 2. Formulation of the Problem

Figure 1 shows gravitactic microorganisms enclosed in a two dimensional rectangular cavity of height  $H$  and width  $L$ , referred to Cartesian coordinates  $(x'_1, x'_2)$ . Microorganisms tend to swim upward at  $(x'_2)$ . In addition, different configuration of discrete temperature are established at bottom and upper wall as shown Figure 1.

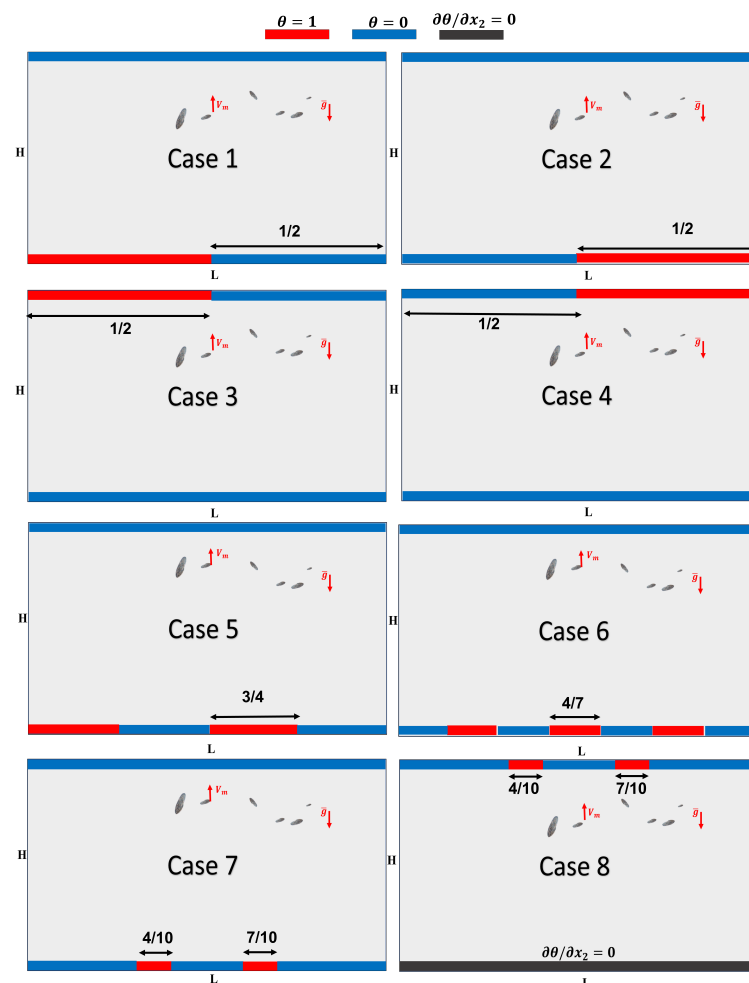


Figure 1. Different heating conditions analyzed in this work.

### 2.1. Dimensionless Equations

The system is governed by the set of Equations (4)–(7), the same coupled-equation-system was used by Alloui et al. [4] and Mil-Martínez et al. [17]. The set of dimensionless parameters are:

$$t = t' \frac{D_m}{H^2}, \quad x_1 = \frac{x'_1}{H}, \quad x_2 = \frac{x'_2}{H}, \tag{1}$$

$$\tilde{u} = u' \frac{H}{D_m}, \quad \tilde{v} = v' \frac{H}{D_m}, \quad \tilde{\omega} = \omega' \frac{H^2}{D_m}, \tag{2}$$

$$\tilde{\Psi} = \frac{\Psi'}{D_m}, \quad \tilde{n} = \frac{n'}{\bar{n}}, \quad \tilde{N} = \frac{\bar{n} - n_b}{n_u - n_b}, \quad \theta = \frac{T - T_h}{T_h - T_c} \tag{3}$$

The dimensionless governing equation are:

$$\frac{\partial^2 \tilde{\Psi}}{\partial x_i^2} = -\tilde{\omega}, \tag{4}$$

$$\frac{\partial \tilde{\omega}}{\partial t} + \tilde{u}_i \frac{\partial \tilde{\omega}}{\partial x_i} = Sc \frac{\partial^2 \tilde{\omega}}{\partial x_i^2} - ScRa \frac{\partial \tilde{n}}{\partial x_1} + LeScRa_T \frac{\partial \theta}{\partial x_1}, \tag{5}$$

$$\frac{\partial \tilde{n}}{\partial t} = -\frac{\partial(\tilde{u}_i + Pe\gamma_2)\tilde{n}}{\partial x_i} + \frac{\partial^2 \tilde{n}}{\partial x_i^2}, \tag{6}$$

$$\frac{\partial \tilde{\theta}}{\partial t} + \tilde{u}_i \frac{\partial \tilde{\theta}}{\partial x_i} = Le \frac{\partial^2 \tilde{\theta}}{\partial x_i^2}, \tag{7}$$

where  $\tilde{u}_i$ ,  $Ra$ ,  $Ra_T$ ,  $Sc$ ,  $\tilde{n}$ ,  $T$ , are the vector velocity, bioconvection Rayleigh number, thermal Rayleigh number, bioconvection Schmidt number, microorganisms concentration and temperature, respectively.  $Pe$ ,  $Le$  and  $\gamma_2$  are the bioconvection Peclet number, Lewis number and a vertical unit vector, respectively. The dimensionless numbers are defined as:

$$\begin{aligned} Ra &= g\bar{n}\vartheta\Delta\rho H^3 / \rho_w \nu D_m \\ Ra_T &= g\beta\Delta TH^3 / \nu\alpha \\ Sc &= \nu / D_m \\ Pe &= \bar{V}_m H / D_m \\ Le &= \alpha / D_m \end{aligned} \tag{8}$$

where  $\alpha$ ,  $g$ ,  $\bar{n}$ ,  $\vartheta$ ,  $\Delta\rho = (\rho_m - \rho_w)$ ,  $\nu$  and  $\bar{V}_m$  are the thermal diffusivity, gravity, dimensional average concentration of microorganisms, microorganisms volume, difference between microorganisms and water density, the kinematic diffusivity, and upward velocity of microorganisms, respectively.

### 2.2. Boundary Conditions

The set of Equations (4)–(7) are subjected to the following boundary conditions: rigid walls are assumed, at both the top and the bottom, and no-slip conditions at side walls. Furthermore, there is no flux of microorganisms through the walls.

$$\tilde{\Psi} = \frac{\partial \tilde{\Psi}}{\partial x_1} = 0, \quad \frac{\partial \tilde{n}}{\partial x_1} = 0 \quad \frac{\partial \theta}{\partial x_1} = 0 \quad \text{at} \quad x_1 = 0, A, \tag{9}$$

$$\tilde{\Psi} = \frac{\partial \tilde{\Psi}}{\partial x_2} = 0, \quad \tilde{n}Pe - \frac{\partial \tilde{n}}{\partial x_2} = 0 \quad \text{at} \quad x_2 = 0, 1, \tag{10}$$

where  $A = L/H$  is the aspect ratio of the cavity. Boundary conditions for temperature along  $x_2$  are shown in Figure 1.

### 3. Numerical Simulations

An Alternating Direction Implicit method (ADI) was used to solve the model governing equations, Equations (4)–(7). A Fortran numerical code was developed using the finite difference method.

#### Code Validation

The numerical code was validated by comparing one case reported by Alloui et al. [6] for  $Ra = 10^3$ ,  $Ra_T = 4 \times 10^3$ ,  $Pe = Sc = Le = 1$  and  $A = 1$ . The results presented in Figure 2 reproduce quantitatively and qualitatively the same iso-patterns of  $\psi$ ,  $n$ , and  $\theta$ , which represent dimensionless streamlines, microorganism concentration and temperature contours, respectively. Note that, heating from below, the microorganisms swim in a clockwise direction, which provokes an accumulation in the upper right corner, generating a deformation of the temperature contours.

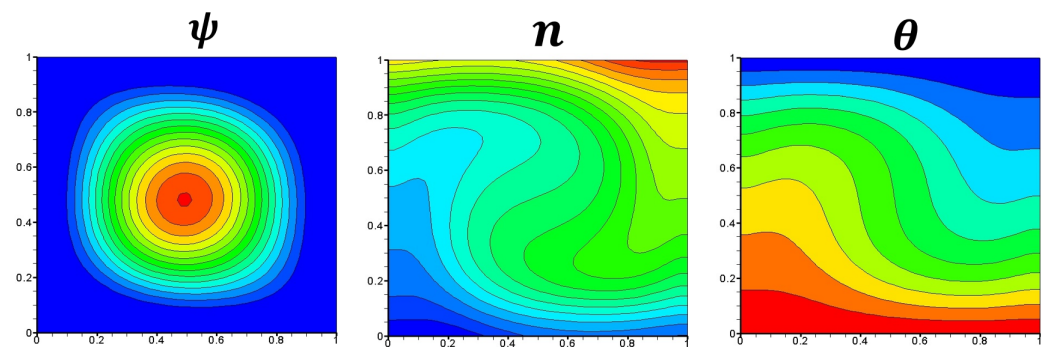


**Figure 2.** From left to right  $\Psi$ ,  $n$ ,  $\theta$ . For  $Ra = 10^3$ ,  $Ra_T = 4 \times 10^3$  and  $Sc = Pe = Le = 1$ .

### 4. Results and Discussion

The results obtained from the numerical simulations are presented in this section. The effect of discrete heat sources, set at different positions in the cavity, on the dynamics of the bioconvective process, is analyzed. Streamlines, concentration and temperature contours of the eight cases are shown. For each result, the thermal Rayleigh ( $Ra_T$ ) was set to 1708 and the bioconvective Rayleigh ( $Ra$ ) was increased until numerical convergence was lost. Case 1: the heat source is located in the left half of the bottom of the cavity as shown in Figure 2. At  $Ra = 100$  a single roll is present in the whole cavity, it depends on the convective process and the concentration of the microorganisms, as can be seen from Figure 3. From  $Ra = 500$  to  $Ra = 1500$  the formation of a cell starts, indicating competition between convective and bioconvective processes. The microorganisms swim from the colder region to accumulate in the warmer region producing concentration plumes, the swimming of microorganisms contributes to thermal diffusion.

Case 2: the heat source is located in the right half of the bottom of the cavity as indicated in Figure 2. At  $Ra = 100$  a single roll is present in the whole cavity in the same way as the case 1. From  $Ra = 500$  to  $Ra = 1500$  the formation of a cell starts, indicating competition between convective and bioconvective processes. However, at  $Ra = 2400$  two well-defined cells of different magnitude were formed, the larger one indicating the swimming of the microorganisms and the smaller the accumulation zone of the microorganisms. The temperature contours are deformed by the swimming of the microorganisms. According to the results reported by Alloui et al. [6], the microorganisms have a uniform distribution preferentially on the right side. This behaviour can be seen in Figure 4.

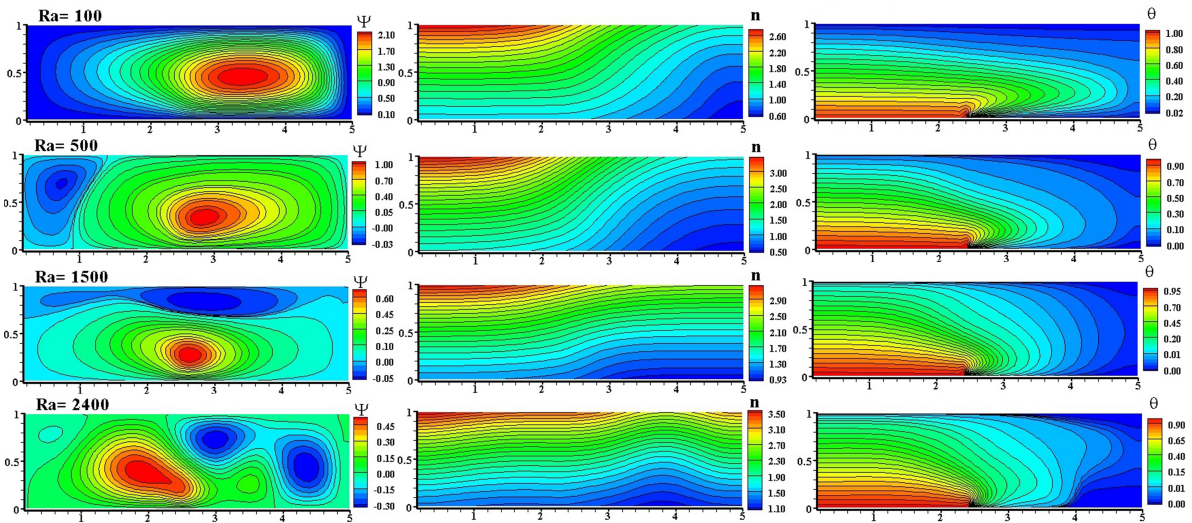


**Figure 3.** Case 1. From left to right, streamlines, microorganisms concentration and dimensionless temperature contours. For  $Sc = 1$ ,  $Pe = 1$ ,  $Ra_T = 1708$  and bioconvective  $Ra$  for 100, 500, 1500 and 2400.

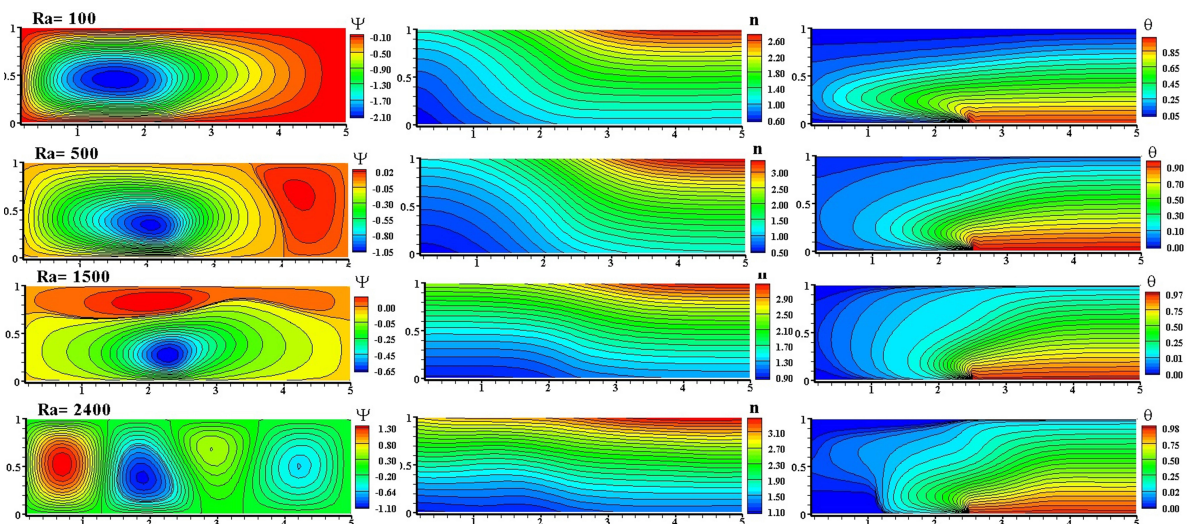


**Figure 4.** Case 2. Streamline, microorganisms concentration and dimensionless temperature contour at left, center and right, respectively.  $Sc = 1$ ,  $Pe = 1$ ,  $Ra_T = 1708$  and bioconvective  $Ra$  for 100, 500, 1500 and 2400.

Case 3: the heat source is located in the left half of the upper wall of the cavity, (see Figure 2). At  $Ra = 100$  a single roll indicates the start of the bioconvective process, due to the absence of buoyancy forces, the temperature contours are affected by this roll, as is presented in Figure 5. At  $Ra = 500$  the formation of a single cell starts, this cell is well-defined at  $Ra = 2300$ , indicating only a bioconvective process. The formation of a concentration plume occurs in the heating zone, almost in the central part. The swimming zone (colder) and the accumulation zone (warmer) are clearly defined. The temperature contours are influenced by the well-defined cell of microorganisms.

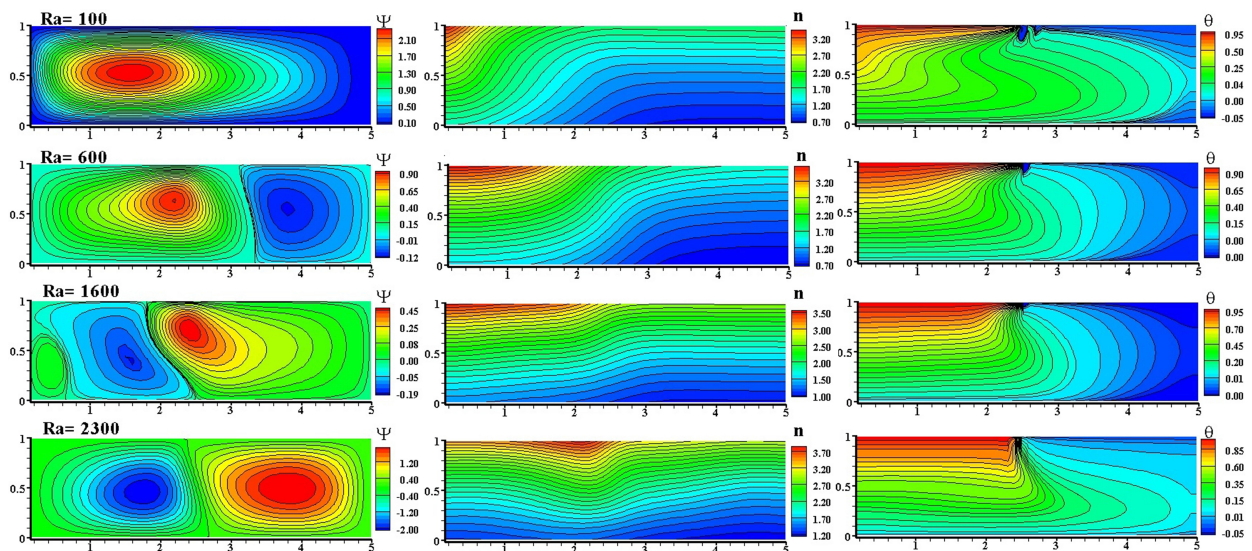


**Figure 5.** Case 3. From left to right, streamlines, microorganisms concentration and dimensionless temperature contours. For  $Sc = 1$ ,  $Pe = 1$ ,  $Ra_T = 1708$  and bioconvective  $Ra$  for 100, 600, 1600 and 2300.

Case 4: the heat source is located in the right half of the upper wall of the cavity, as is presented in Figure 2. The results are very similar to the previous case, a well-defined cell is depicted, the temperature contours are affected by the cell; however, in this case the concentration plume is not found (see Figure 6). One explanation is that, although the cell is well defined, it is also deformed, these deformations affect the formation of the plume.

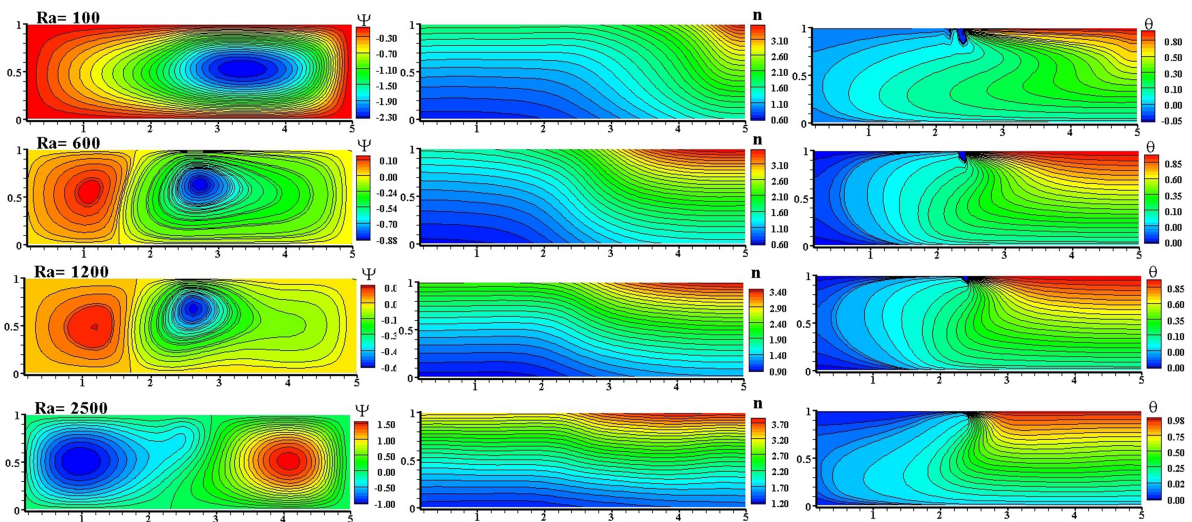


**Figure 6.** Case 4. From left to right, streamlines, microorganisms concentration and dimensionless temperature contours. For  $Sc = 1$ ,  $Pe = 1$ ,  $Ra_T = 1708$  and bioconvective  $Ra$  for 100, 600, 1200 and 2500.

Case 5: two non-symmetrical heat sources are placed at the bottom of the cavity (see Figure 2). At  $Ra = 100$ , two cells partially are present, the microorganisms are concentrated on the upper wall of the cavity, the temperature distribution is well defined around the sources. In the range of  $Ra = 2200$  to  $Ra = 3600$ , the temperature distribution is affected the bioconvective process, the microorganisms form two concentration plumes ending in three. During this process a cell is defined which confirms that the swimming of microorganisms takes place in the cooler zone to concentrate in the warmer zone (Figure 7).

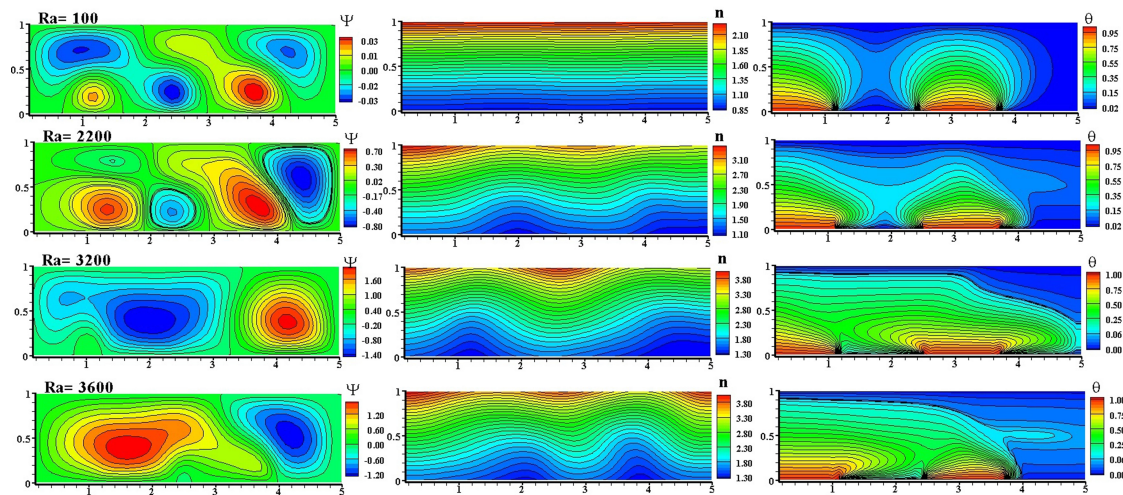


**Figure 7.** Case 5. From left to right, streamlines, microorganisms concentration and dimensionless temperature contours. For  $Sc = 1$ ,  $Pe = 1$ ,  $Ra_T = 1708$  and bioconvective  $Ra$  for 100, 2200, 3200 and 3600.

Case 6: three symmetrically heat sources are set alternately at the bottom of the cavity, (as shown in Figure 2). At  $Ra = 100$ , three partially-defined cells are presented, a higher concentration of microorganisms is located in the center of the top wall, and the temperature distribution is uniform in the cavity. In the range of  $Ra = 500$  to  $Ra = 1200$ , three cells of microorganisms are defined, corresponding to each heat source, increasing the concentration of micro-organisms in the center. Finally at  $Ra = 2200$ , the temperature distribution is affected due to the increased concentration of microorganisms, corresponding to a single distorted cell. This cell is due to a high concentration of microorganisms in the cavity, they seek the most suitable structure and swimming direction, (see Figure 8).

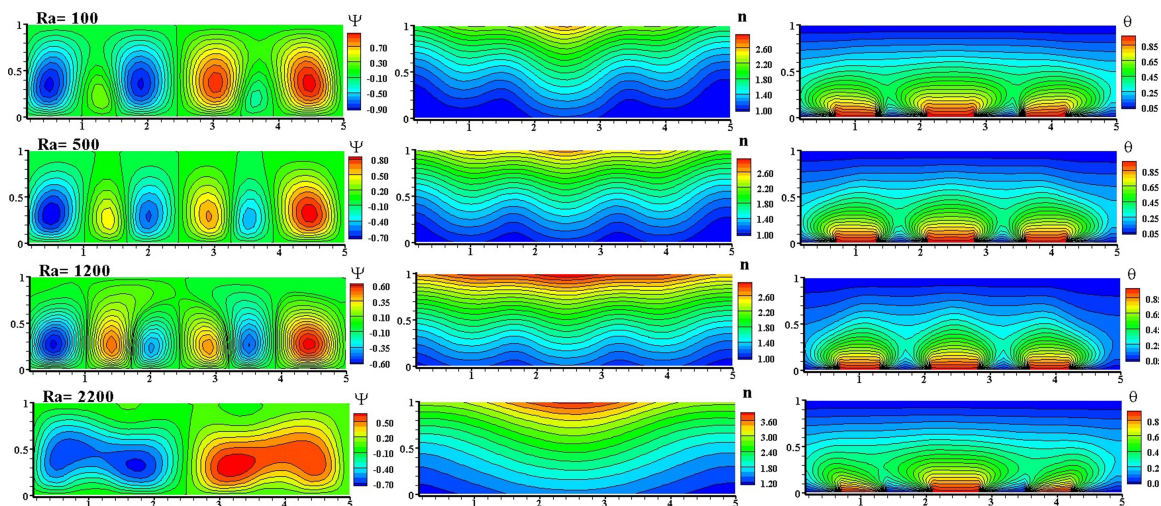


**Figure 8.** Case 6. From left to right, streamlines, microorganisms concentration and dimensionless temperature contours. For  $Sc = 1$ ,  $Pe = 1$ ,  $Ra_T = 1708$  and bioconvective  $Ra$  for 100, 500, 1200 and 2200.

Case 7: two symmetrical heat sources are placed at the bottom of the cavity, as is presented in Figure 2. Two well-defined cells are formed together with the two thermal plumes, corresponding to each heat source, and the temperature distribution is uniform. In the range of  $Ra = 1900$  to  $Ra = 2300$ , the two cells and thermal plumes remain and show distortions, due to the increase of microorganisms concentration, which substantially affects the temperature distribution, (see Figure 9).

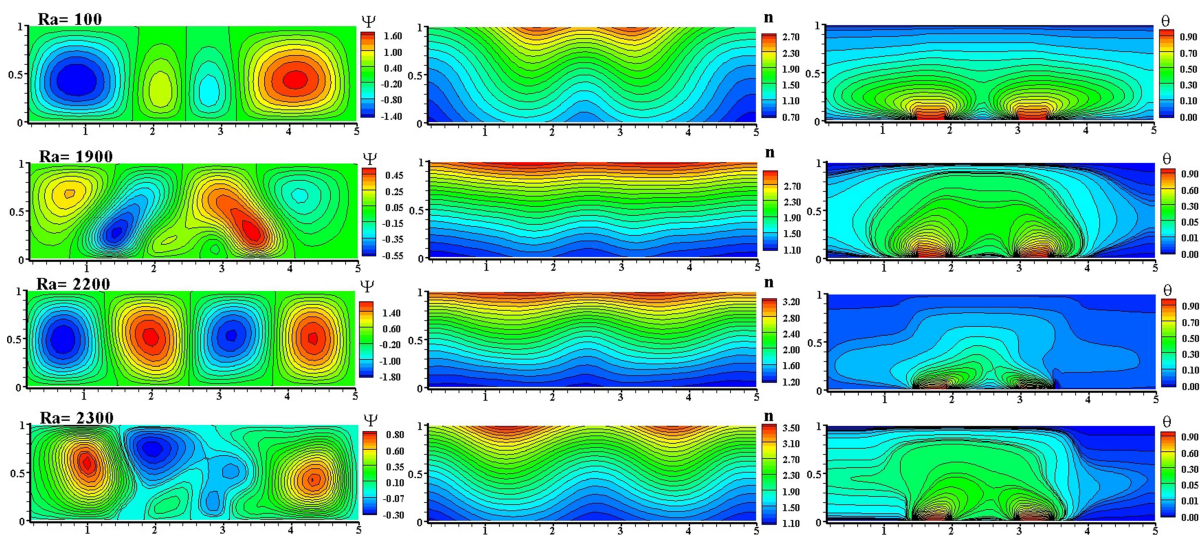


**Figure 9.** Case 7. From left to right, streamlines, microorganisms concentration and dimensionless temperature contours. For  $Sc = 1$ ,  $Pe = 1$ ,  $Ra_T = 1708$  and bioconvective  $Ra$  for 100, 1900, 2200 and 2300.

Case 8: two symmetrical heat sources are placed at the top, in addition an adiabatic condition is set at the bottom, as indicated in Figure 2. In the range of  $Ra = 1700$  to  $Ra = 2000$ , the increased concentration of microorganisms generates two or even three cells, because the microorganisms look for the best arrangement that defines the swimming and accumulation zones. The swimming dynamics of the microorganisms affects the temperature distribution. The adiabatic condition in the wall generates another temperature distribution in the cavity, which affect cell formation because the dynamics of the microorganisms seek out the cooler zones to swim to the surface and accumulate in the warmer zones, see Figure 10.

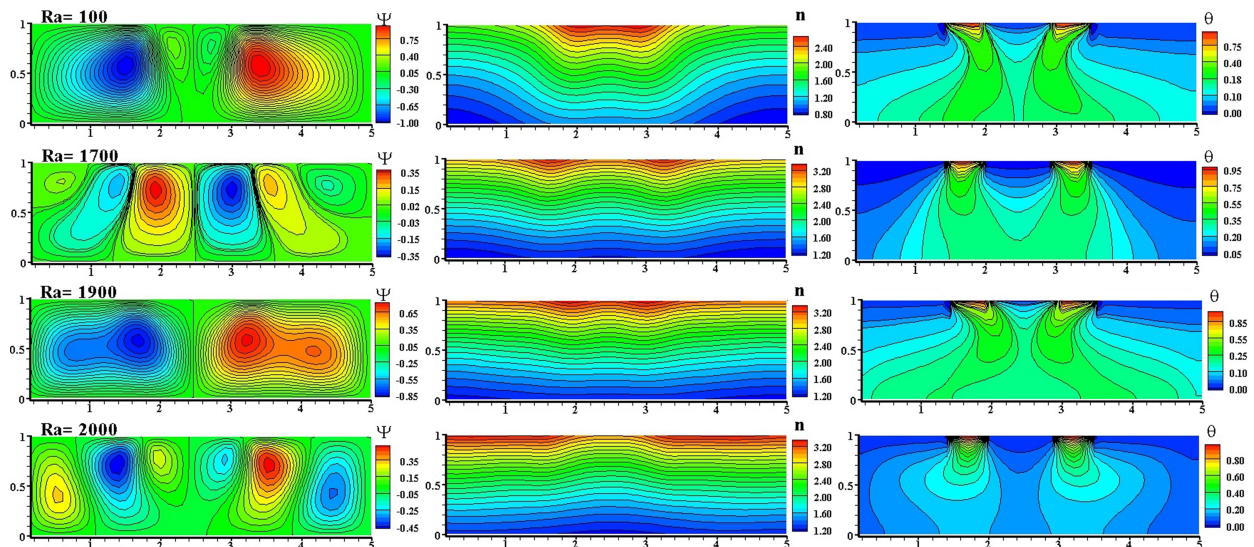


**Figure 10.** Case 8. From left to right, streamlines, microorganisms concentration and dimensionless temperature contours. For  $Sc = 1$ ,  $Pe = 1$ ,  $Ra_T = 1708$  and bioconvective  $Ra$  for 100, 1700, 1900 and 2000.

## 5. Conclusions

Numerical simulations were performed to analyze the effect of discrete heat sources, placed at different positions in the cavity, on the dynamics of the bioconvective process. The principal findings are briefly described as:

- The numerical code developed for this work was validated with results published in the specialized literature.
- At low  $Ra$  numbers the driving force of the convective process are the thermal sources, and increasing  $Ra$  produces the start of the bioconvective process.
- The number of cells generated in the convective process depends on the number of heat sources and the concentration of microorganisms, this concentration should not be high.
- For high  $Ra$  values, a single cell is generated because the microorganisms look for the most suitable and efficient way to reach the surface.
- The temperature distribution in the cavity depends on the concentration of microorganisms.
- It is determined that microorganisms swim in colder regions to reach the surface and accumulate in warmer regions, i.e., close to the heating sources.
- Considering adiabatic conditions, which for this work was the bottom wall, directly influences the temperature distribution, which in turn impacts the dynamics of the bioconvective process.
- Wavelength of the concentration contour is related to the number of rolls, as is depicted on results of Alloui et al. [6] and Mil-Martínez et al. [17]. In all cases the heating sources affect the wavelength of concentration contour.
- The control of microorganisms distribution can be used in bioprocess to separate contaminants, and to analyze the heat transfer dissipation in micro and nanodevices.
- These results can be applied to control and understand the dynamics of microorganisms with discrete heat sources.

**Author Contributions:** Conceptualization, R.M.-M. and R.O.V.; methodology, R.M.-M., R.O.V., J.P.E. and I.P.-R.; software, R.M.-M.; validation, R.M.-M., R.O.V., J.P.E., I.P.-R., M.T., A.G.-L. and F.L.-S.; formal analysis, R.M.-M., R.O.V., J.P.E., I.P.-R., M.T., A.G.-L. and F.L.-S.; investigation, R.M.-M., R.O.V., J.P.E., I.P.-R., M.T., A.G.-L. and F.L.-S.; resources, R.O.V. and J.P.E.; data curation, R.M.-M.; writing—original draft preparation, R.M.-M., R.O.V., J.P.E., I.P.-R., M.T., A.G.-L. and F.L.-S.; writing—review and editing, R.M.-M., R.O.V., J.P.E., I.P.-R., M.T., A.G.-L. and F.L.-S.; visualization, R.M.-M. and R.O.V.; supervision, R.M.-M. and R.O.V.; project administration, R.M.-M., R.O.V. and J.P.E.; funding acquisition, R.O.V. and J.P.E. All authors have read and agreed to the published version of the manuscript.

**Funding:** The authors R.O.V. and J.P.E. would like to acknowledge the financial support SIP-IPN 20221783 and SIP-IPN 20221572. F.L.-S. gratefully acknowledges support by UNAM, DGAPA (PAPIIT IN112221).

**Acknowledgments:** RMM gratefully acknowledges support by National System of Researchers (SNI) of México and Major Daniel Limón Torres for endorsing this work.

**Conflicts of Interest:** The authors declare no conflict of interest.

## Nomenclature

$A$	Aspect ratio	-
$D_m$	Diffusivity of microorganisms	$\text{m}^2\text{s}^{-1}$
$g$	Gravity	$\text{ms}^{-2}$
$H$	Cavity height	m
$\tilde{j}$	Dimensionless flux of microorganisms	$\text{cellm}^{-2}\text{s}^{-1}$
$L$	Cavity width	m
$Le$	Lewis number	-
$n$	Microorganism concentration	$\text{cellm}^{-3}$
$n_b$	Bottom concentration of microorganisms	$\text{cellm}^{-3}$

$n_u$	Upper concentration of microorganisms	$\text{cellm}^{-3}$
$\bar{n}$	Average concentration of microorganisms	$\text{cellm}^{-3}$
$\bar{N}$	Average dimensionless concentration of microorganisms	-
$Pe$	Peclet number	-
$Ra$	Rayleigh number	-
$Sc$	Schmidt number	-
$t$	Dimensionless time	-
$T$	Temperature	$^{\circ}\text{C}$
$T_c$	Cold wall temperature	$^{\circ}\text{C}$
$T_h$	Hot wall temperature	$^{\circ}\text{C}$
$\tilde{u}$	Horizontal component of dimensionless velocity	$\text{ms}^{-1}$
$\tilde{v}$	Vertical component of dimensionless velocity	$\text{ms}^{-1}$
$\tilde{V}_c$	Upward microorganisms' velocity	$\text{ms}^{-1}$
$x_1, x_2$	Dimensionless coordinate system	-
<b>Greek symbols</b>		
$\alpha$	Thermal diffusivity	$\text{m}^2\text{s}^{-1}$
$\vartheta$	Volume of microorganisms	$\text{m}^3$
$\gamma$	Unit vertical vector	-
$\Psi$	Dimensionless stream function	-
$\tilde{\omega}$	Dimensionless vorticity	-
<b>Superscripts</b>		
<i>sub</i>	Subcritical	
<i>sup</i>	Supercritical	
'	Dimensional variable	

### Abbreviations

The following abbreviation is used in this manuscript:

ADI Alternating Direction Implicit

### References

- Rashad, A.M.; Nabwey, H.A. Gyrotactic mixed bioconvection flow of a nanofluid past a circular cylinder with convective boundary condition. *J. Taiwan Inst. Chem. Eng.* **2019**, *99*, 9–17. [[CrossRef](#)]
- Kuznetsov, A.V. The onset of bioconvection in a suspension of negatively geotactic microorganisms with high-frequency vertical vibration. *Int. Commun. Heat Mass Transf.* **2005**, *32*, 1119–1127. [[CrossRef](#)]
- Kuznetsov, A.V. Thermo-bioconvection in a suspension of oxytactic bacteria. *Int. Commun. Heat Mass Transf.* **2005**, *32*, 991–999. [[CrossRef](#)]
- Alloui, Z.; Nguyen, T.H.; Bilgen, E. Stability analysis of thermo-bioconvection in suspensions of gravitactic microorganisms in a fluid layer. *Int. Commun. Heat Mass Transf.* **2006**, *33*, 1198–1206. [[CrossRef](#)]
- Nield, D.A.; Kuznetsov, A.V. The onset of bio-thermal convection in a suspension of gyrotactic microorganisms in a fluid layer: Oscillatory convection. *Int. J. Therm. Sci.* **2006**, *45*, 990–997. [[CrossRef](#)]
- Alloui, Z.; Nguyen, T.H.; Bilgen, E. Numerical investigation of thermo-bioconvection in a suspension of gravitactic microorganisms. *Int. J. Heat Mass Transf.* **2007**, *50*, 1435–1441. [[CrossRef](#)]
- Taheri, M.; Bilgen, E. Thermo-bioconvection in a suspension of gravitactic micro-organisms in vertical cylinders. *Int. J. Heat Mass Transf.* **2008**, *51*, 3535–3547. [[CrossRef](#)]
- Niu, J.; Fu, C.; Tan, W. Thermal convection of a viscoelastic fluid in an open-top porous layer heated from below. *J. Non-Newton. Fluid Mech.* **2010**, *165*, 203–211. [[CrossRef](#)]
- Kuznetsov, A. Bio-thermal convection induced by two different species of microorganisms. *Int. Commun. Heat Mass Transf.* **2011**, *38*, 548–553. [[CrossRef](#)]
- Xun, S.; Zhao, J.; Zheng, L.; Zhang, X. Bioconvection in rotating system immersed in nanofluid with temperature dependent viscosity and thermal conductivity. *Int. J. Heat Mass Transf.* **2017**, *111*, 1001–1006. [[CrossRef](#)]
- Khan, M.; Irfan, M.; Khan, W. Impact of nonlinear thermal radiation and gyrotactic microorganisms on the Magneto-Burgers nanofluid. *Int. J. Mech. Sci.* **2017**, *130*, 375–382. [[CrossRef](#)]
- Ramzan, M.; Chung, J.D.; Ullah, N. Radiative magnetohydrodynamic nanofluid flow due to gyrotactic microorganisms with chemical reaction and non-linear thermal radiation. *Int. J. Mech. Sci.* **2017**, *130*, 31–40. [[CrossRef](#)]
- Saini, S.; Sharma, Y.D. Analysis of onset of bio-thermal convection in a fluid containing gravitactic microorganisms by the energy method. *Chin. J. Phys.* **2018**, *56*, 2031–2038. [[CrossRef](#)]

14. Zhao, M.; Xiao, Y.; Wang, S. Linear stability of thermal-bioconvection in a suspension of gyrotactic micro-organisms. *Int. J. Heat Mass Transf.* **2018**, *126*, 95–102. [[CrossRef](#)]
15. Saini, S.; Sharma, Y.D. Numerical study of nanofluid thermo-bioconvection containing gravitactic microorganisms in porous media: Effect of vertical throughflow. *Adv. Powder Technol.* **2018**, *29*, 2725–2732. [[CrossRef](#)]
16. Belabid, J.; Allali, K. Thermo-bioconvection in horizontal porous annulus with the presence of phototactic microorganisms. *Int. J. Eng. Sci.* **2019**, *140*, 17–25. [[CrossRef](#)]
17. Mil-Martínez, R.; Ferrer, V.; Turcio, M.; López-Serrano, F.; Ortega, J.; Vargas, R. Stability analysis and numerical simulation of gravitactic bioconvection in a rectangular cavity. *Comput. Math. Appl.* **2019**, *77*, 222–236. [[CrossRef](#)]